Modeling the dynamics of human hair cycles by a follicular automaton

J. Halloy*, B. A. Bernard†, G. Loussouarn‡, and A. Goldbeter*§

*Faculté des Sciences, Université Libre de Bruxelles, Campus Plaine, C.P. 231, B-1050 Brussels, Belgium; †Groupe ''Biologie du Cheveu'', Centre de Recherche C. Zviak, L'Oréal, 90 rue du Général Roguet, F-92110 Clichy, France; and ‡Laboratoires de Recherche Appliquée et Développement, L'Oréal, 66 rue Henri Barbusse, F-92110 Clichy, France

Communicated by I. Prigogine, Free University of Brussels, Brussels, Belgium, May 15, 2000 (received for review December 23, 1999)

The hair follicle cycle successively goes through the anagen, catagen, telogen, and latency phases, which correspond, respectively, to hair growth, arrest, shedding, and absence before a new anagen phase is initiated. Experimental observations collected over a period of 14 years in a group of 10 male volunteers, alopecic and nonalopecic, allowed us to determine the characteristics of scalp hair follicle cycles. On the basis of these observations, we propose a follicular automaton model to simulate the dynamics of human hair cycles. The automaton model is defined by a set of rules that govern the stochastic transitions of each follicle between the successive states anagen, telogen, and latency, and the subsequent return to anagen. The transitions occur independently for each follicle, after time intervals given stochastically by a distribution characterized by a mean and a variance. The follicular automaton model accounts both for the dynamical transitions observed in a single follicle and for the behavior of an ensemble of independently cycling follicles. Thus, the model successfully reproduces the evolution of the fractions of follicle populations in each of the three phases, which fluctuate around steady-state or slowly drifting values. We apply the follicular automaton model to the study of spatial patterns of follicular growth that result from a spatially heterogeneous distribution of parameters such as the mean duration of anagen phase. When considering that follicles die or miniaturize after going through a critical number of successive cycles, the model can reproduce the evolution to hair patterns similar to well known types of diffuse or androgenetic alopecia.

human scalp hair | hair follicle cycles | automaton model | alopecia

Human hair represents an ensemble of some 10^5 hair follicles that continually evolve over the course of time. At any moment, a follicle is either growing (anagen or A phase) or ceasing to grow and involuting (catagen or C phase) but still on the scalp (telogen or T phase) before shedding and entering a new cycle. These successive phases constitute a follicular cycle (1–4). The duration of such a cycle is variable but typically ranges from a few months to several years (5, 6). Each follicle can undergo repeated cycles until it eventually dies or miniaturizes to give rise to a vellus hair (7, 8); the vellus hair shaft is not pigmented and has a cross-sectional diameter much shorter than normal (9). Whether miniaturization (M) occurs progressively or abruptly is still unclear. If a large proportion of follicles die or miniaturize, alopecia—balding—ensues, with a severity that depends on the location of lost follicles (10) and on the amount of total hair that is irreversibly shed.

The most comprehensive data on the human hair cycle were provided by a study carried out over a period of 14 years in a group of 10 normal and alopecic male volunteers (5, 6, 11). The data were collected by using the phototrichogram technique, which allowed determining the duration of A and T phases of each follicle from a 1-cm^2 scalp area where about 100 follicles have been identified. Although this method cannot catch the C phase, which is too brief, it permits the quantification of the latency (L) phase that follows hair shedding and precedes the onset of the next A phase (5). For each subject, two photographs of the same area were taken once a month at a 2-day interval for 144 successive months. This protocol (5) enabled the exact counting of hairs in the A, T, or L phase. The data provide for a group of subjects the detailed timing of transitions between these three follicular phases over more than a decade. About 9,000 hair cycles were thus recorded and characterized for a total of about 930 hair follicles followed monthly.

The availability of such an informative body of data on successive follicular cycles for normal and alopecic subjects allowed us to investigate the short- and long-term dynamics of the human hair cycle by using a theoretical model based on the experimental data. This model, designed to reproduce the dynamics of human hair cycles, is an automaton model that simulates stochastic transitions between the successive phases of the follicular cycle. The model belongs to the class of "cellular automata," which are often used to study the spatiotemporal dynamics of biological systems by means of computer simulations (12). Because we focus on the follicular cycle, we refer to this model as the "follicular automaton."

The follicular automaton model first is used to simulate the time evolution of the distribution of scalp hair follicles in the A, T, and L phases. The results obtained for nonalopecic and alopecic subjects are compared. By including the death or M of a follicle after a critical number of hair cycles, we apply the follicular automaton model to the spatiotemporal evolution of an ensemble of cycling follicles to investigate the conditions in which patterns of androgenetic alopecia in men (10) or diffuse alopecia in women (13) develop over the course of time.

Modeling the Dynamics of Human Hair Cycles: The Follicular Automaton. We represent the hair cycle as the succession of the A, T, and L phases (5). The C phase is relatively brief (less than 1 month) and cannot be distinguished from T phase by the phototrichogram method; therefore, it will be lumped into the longer T phase. The follicular automaton (schematized in Fig. 1) remains in a given phase during a variable interval of time, after which it moves to the next phase. The automaton completes a cycle when entering a new A phase. Follicular death or M can be included in the model by adding a transition from state T that removes the follicle from its cycle. From the bulk of data on volunteers involved in the experimental study on which the present model is based, the latter transition was found to be negligible; thus, it will not be considered in most of the following.

The follicular automaton model will be treated in a stochastic manner. Each follicle in a field of hair follicles is characterized by (*i*) its spatial position, (*ii*) its state (phase A, T, L, or M), (*iii*) the time to the next transition, and (*iv*) the number of cycles

Abbreviations: A, anagen; C, catagen; T, telogen; L, latency; M, miniaturization.

§To whom reprint requests should be addressed. E-mail: agoldbet@ulb.ac.be.

The publication costs of this article were defrayed in part by page charge payment. This article must therefore be hereby marked "*advertisement*" in accordance with 18 U.S.C. §1734 solely to indicate this fact.

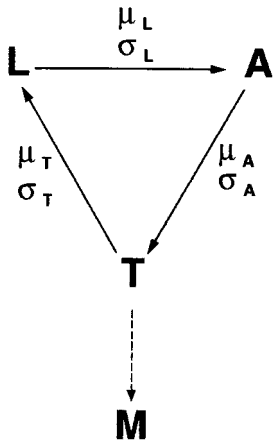

Fig. 1. The follicular automaton. The figure represents the transition of a model follicle from A to T and to L phase, successively. After phase T, the follicle may die, miniaturize [transition to M; this transition (dashed arrow) may happen after some critical number of cycles], or enter a new L phase. In this stochastic model, the values of the duration of the A, T, and L phases are given by distributions characterized by mean values μ_A, μ_T, and μ_L and by variances σ_A, σ_T, and σ_L. The time evolution generated by the follicular automaton is obtained numerically by following the procedure described in the text.

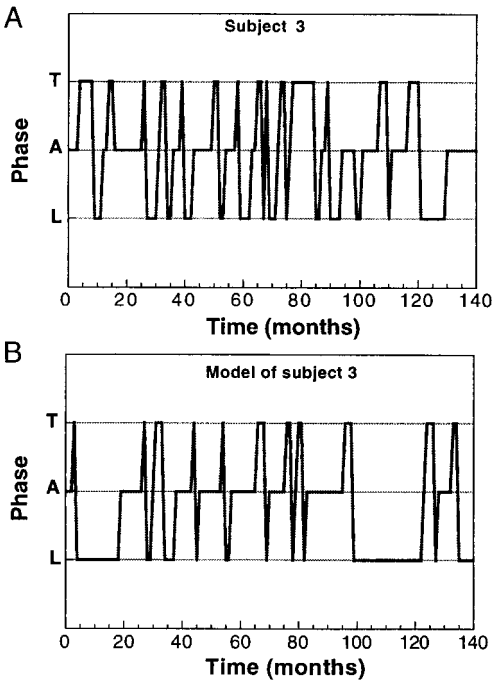

Fig. 3. Typical sequence of transitions between A, T, and L phases for a single follicle, as observed for subject 3 (see also Fig. 4*C*) of the experimental study (*A*) and generated by the follicular automaton model by using Eq. **1** (*B*). For the three duration distributions, the values considered for the mean and variance, determined from the experimental data, are (in months) $\mu_A = 6.49$, $\sigma_A = 10.16$, $\mu_T = 2.17$, $\sigma_T = 1.11$, $\mu_L = 4.56$, and $\sigma_L = 9.57$.

performed since entering the first A phase. Given that the measurements were performed for a limited number of hair cycles on any given volunteer, typically 10 successive cycles on average for 100 follicles, the duration of the different phases fluctuates significantly from cycle to cycle. We shall refer below to three typical subjects, designated 1, 2, and 3, who correspond, respectively, to subjects A, F, and G of the experimental study (5).

Subject 1 is nonalopecic, whereas subjects 2 and 3 are alopecic according to Hamilton's scale (10). Fig. 2 *A–C* shows the duration of phases A, T, and L measured over 144 successive months on subject 1. These data indicate that the duration of the phases (in months) fluctuates around mean values of 16.9, 1.8, and 5.2 for phases A, T, and L, respectively; for both phases A and L, the variance is of the order of the mean, but it is relatively low with respect to the mean for the T phase. For subjects 2 and 3, the corresponding mean values for phases A, T, and L are (in months) 5.12 and 6.49, 2.09 and 2.17, and 3.53 and 4.56,

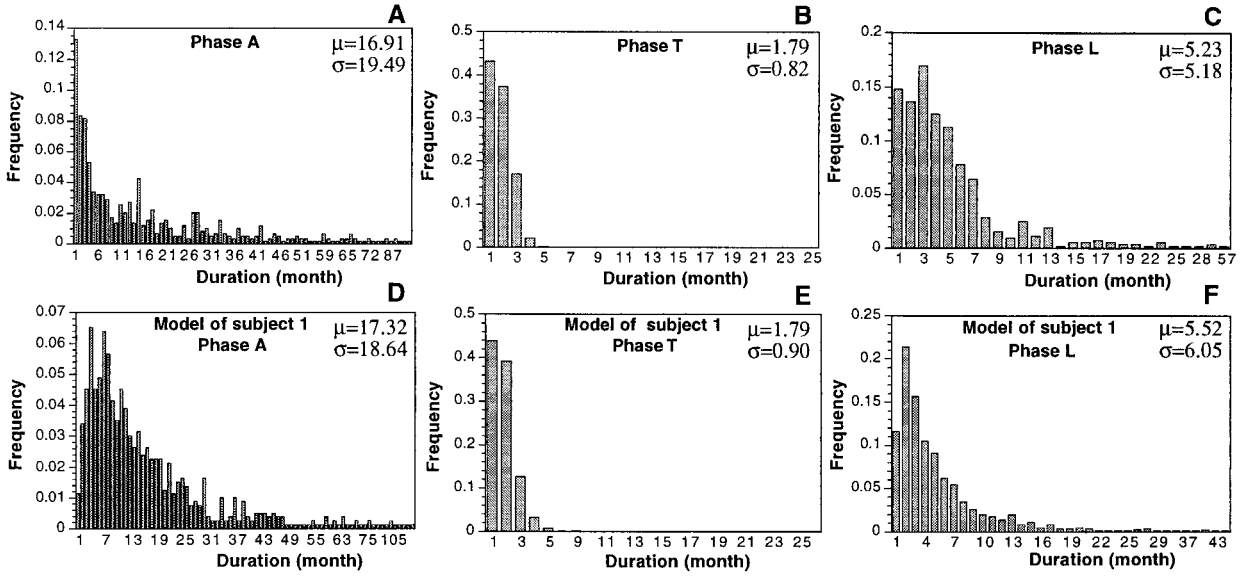

Fig. 2. Histograms of the durations of A, T, and L phases. (*A–C*) Experimental data obtained for subject A (referred to herein as subject 1) in the experimental study of Courtois *et al.* (5). (*D–F*) Histograms obtained theoretically by means of log-normal distribution (Eq. **1**) for 100 follicles followed during 144 months, when using, for each phase, the mean value and the variance as determined and indicated in *A*, *B*, or *C*. The mean value and variance predicted by the model are indicated in *D–F*.

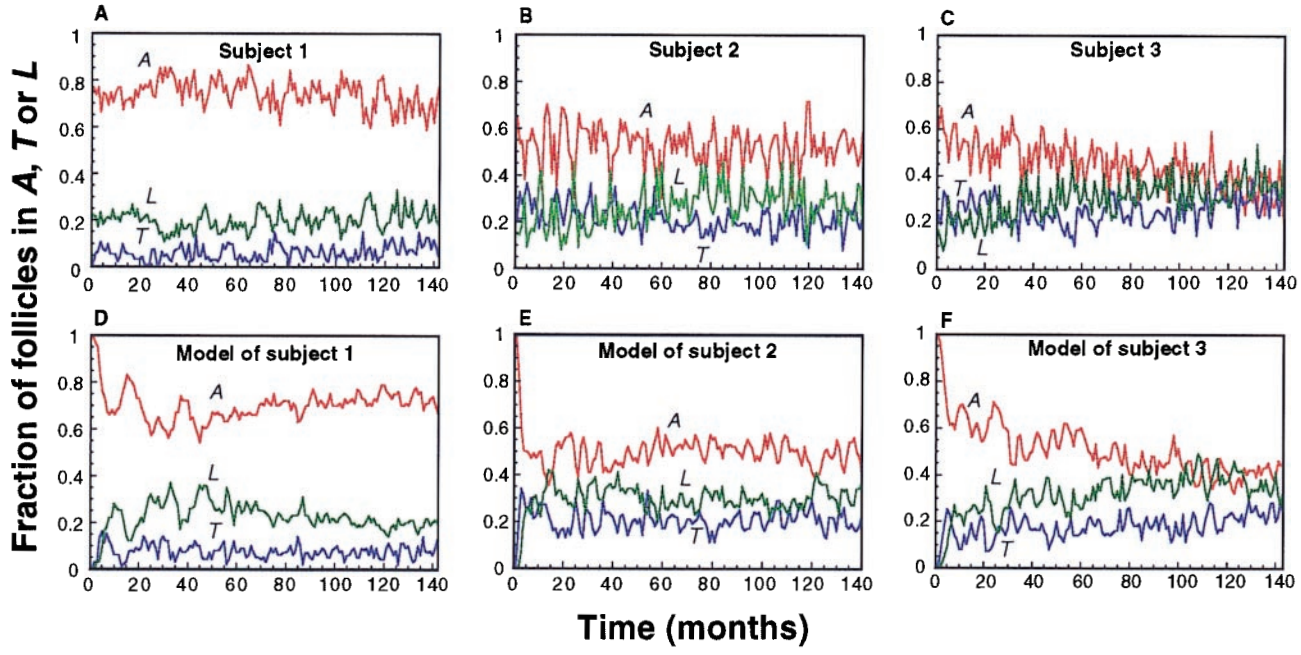

Fig. 4. Proportions of follicles in A, T, and L phases. The experimental data have been obtained for nonalopecic subject 1 (*A*) and for alopecic subjects 2 (*B*) and 3 (*C*) (see text). The corresponding theoretical curves, shown in *D–F*, are generated by the follicular automaton, taking for the mean and variance in Eq. **1** the values determined from the corresponding experimental data in *A–C*. These values, for subject 1, are those given in the legend to Fig. 2, and for subject 2, the values are $\mu_A = 5.16$, $\sigma_A = 4.50$, $\mu_T = 2.09$, $\sigma_T = 1.06$, $\mu_L = 3.53$, and $\sigma_L = 5.43$; the values for subject 3 are specified below. In contrast to what is observed for subjects 1 and 2, for subject 3, the data indicate a continuous drift in the values of the three follicular fractions over the course of time. The initial conditions in *D–F* correspond to a situation in which 100 (independent) follicles start in A phase. In *F* (subject 3), the theoretical curve is generated by assuming a progressive decrease in the mean duration of A phase, by 1-month decrements, from an initial value of 10 months to 4 months at the end of the time period considered, i.e., 144 months, according to the equation $\mu_A = \mu_{Ai}[n^*/(n^* + <n>)]$, with $n^* = 6$ and $\mu_{Ai} = 10$ months; $<n>$ represents the mean number of cycles performed by the 100 follicles considered. The mean value and variance of the T and L duration distributions for subject 3 are the same as given in Fig. 3.

respectively (see legends to Fig. 3 and 4). The mean duration of the A phase is thus much shorter for the alopecic subjects (5).

We have chosen to represent the distribution of the durations of each follicular phase by a log-normal function:

$$f(x;\,\mu,\,\sigma) = \frac{1}{x\sqrt{2\pi\sigma}}\exp\left[-\frac{1}{2\sigma^2}(\log x - \mu)^2\right] \qquad [1]$$

where x is the duration, and μ and σ are, respectively, the mean and variance of the distribution of durations for a given phase. The three phases generally differ by the values of μ and σ. For simulations with the follicular automaton, we have taken for μ and σ the values calculated from experimental data for each phase and subject. The choice of a log-normal distribution stems from the fact that, in agreement with experimental observations, this positively defined function is skewed toward small durations but still presents a long tail corresponding to durations that are long with respect to the mean. Other distributions, such as the exponential one, would likely lead to similar results.

Fig. 2 *D–E* shows histograms generated by the model for the parameters of subject 1, when considering a reduced number of follicles (about 100), as in the experimental study. Because the simulations are carried out (*i*) with a limited number of follicles, (*ii*) during a finite time, and (*iii*) by drawing random numbers distributed according to Eq. **1**, the theoretical distributions give mean values and variances close (but not identical) to the experimental ones, even though the experimental values of μ and σ were used in Eq. **1**. The main difference between the theoretical and experimental distributions is that the weight of small durations (1 to 2 months) is underevaluated in the model, because the log-normal function tends to vanish when the duration x approaches zero. Despite this difference, as shown below, the follicular automaton model successfully accounts for many of the experimentally determined properties of hair cycles.

The evolution of a field of cycling follicles is obtained by iterating the following steps, assuming that all follicles evolve independently from one another. (Step 1) We begin by fixing the initial conditions, i.e., the state (A, T, or L) of each follicle. The initial number of cycles is set equal to zero. The time interval to the next transition in the cycle A → T → L → A is determined randomly for each follicle according to the distribution of durations given for each phase by Eq. **1**. (Step 2) At each time step (equal to 1 month), the time to the next transition is reduced by 1 month. Each follicle is tested to determine whether the time has come to undergo a transition to the next phase in the cycle. For the follicles that undergo such a transition, a time interval to the next transition in the cycle is again determined randomly according to the distribution of durations given for the new phase by Eq. **1**. As soon as the follicle enters a new A phase, the count of cycles increases by one. (Step 3) At each time step, we determine the number of follicles in phase A, T, or L as well as other characteristics such as the mean number of cycles performed by follicles in the area considered. The algorithm returns to step 2 until the specified end of the simulation is reached.

The procedure outlined above allows us to include additional properties. Thus, it is possible to consider the effect of a variation of some parameters of the model over the course of time, such as the mean duration of the A, T, and/or L phases. Then, depending on the mean number of cycles performed, the values of the mean durations μ_A, μ_T, and/or μ_L in Eq. **1** are increased or decreased. Similarly, changes in the variances σ_A, σ_T, and/or σ_L with time can also be considered. Moreover, for long-term evolutions, the follicles can exit the cycle by dying or miniatur-

izing and being trapped in state M (see Fig. 1) after passing through a critical number of cycles, e.g., 25.

Before turning to the collective dynamics of a field of cycling follicles, it is useful to compare the time evolution of a given follicle in the experimental study and in the stochastic model. Fig. 3*A* illustrates the transitions observed over the whole course of the experimental study for one particular follicle of alopecic subject 3. Fig. 3*B* shows the transitions generated by the follicular automaton model when inserting into Eq. **1** the values of μ and σ calculated for each phase from the experimental data for this subject. Comparing the two curves indicates that the model generates a time course that captures the essential features of the transitions between A, T, and L phases. The trace in Fig. 3*A* shows that the transition from T to L can sometimes be missed in the experiments, because the duration of the L phase can be shorter than 1 month, which is the interval between successive measurements. In the model, the direct jump from T to A will not occur, because the minimum duration of each of the three phases is set equal to 1 month and because the sequence of transitions A $\rightarrow$ T $\rightarrow$ L is imposed.

Distribution of Hair Follicles in the Different Phases. The relative proportions of hair follicles in A, T, and L phases provide a signature of the general state of hair for a given individual. Fig. 4 *A–C* shows the time evolution of the fractions of follicles in the three phases as recorded for nonalopecic subject 1 and alopecic subjects 2 and 3. In Fig. 4 *A* and *B*, the fractions fluctuate around a roughly constant level; however, in Fig. 4*C*, the fraction of A follicles progressively decreases, whereas the fractions in the T and L phases concomitantly increase with time. The data indicate that the fraction of A follicles is significantly larger for subject 1 compared with that of subjects 2 and 3. This difference results from the fact that the mean duration of A phase is longer for the nonalopecic subject. Moreover, the fraction of T follicles is higher for subjects 2 and 3 versus subject 1.

Fig. 4 *D–F* presents simulations of the follicular automaton model corresponding to subjects 1–3, respectively; the experimental time evolution of the fractions of hair follicles in the A, T, and L phases in these subjects is represented in Fig. 4 *A–C*. The values of μ_A, μ_T, and μ_L considered in Eq. **1** are equal to the mean values of the durations of A, T, and L phases as determined from experimental observations on these subjects. In the simulations, all of the 100 follicles considered are taken initially as being in A phase. Very quickly, the fractions evolve toward a level around which they fluctuate, similarly to what is observed experimentally. This level is roughly constant for subjects 1 and 2, but it changes over the course of time for subject 3. To a large degree, the follicular automaton model reproduces the qualitative and quantitative characteristics that differentiate the three individuals compared in Fig. 4 *A–C*. Because of the stochastic nature of the model, another simulation would give a similar, although not identical, evolution of the three fractions for each individual. The stochastic follicular automaton is capable of accounting for the observation that the fraction of follicles in each of the three phases fluctuates around a mean level.

The results of Fig. 4 show that the follicular automaton reproduces well the observations pertaining to subjects 1, 2, and 3. The model also provides excellent agreement with the observations collected for the other seven subjects of the experimental study (5) when inserting into Eq. **1** the values of the parameters derived for these subjects in the manner described in Fig. 2 (data not shown).

Spatiotemporal Dynamics of Hair Cycles and Alopecia. The long-term development of human hair on the scalp proceeds in a heterogeneous manner. This phenomenon is reflected by the age-related appearance of scalp areas where follicular growth progressively stops, resulting in scarcity or even disappearance of hair follicles (10, 14). In men, vertex and "temporal gulfs" are particularly affected (10), whereas in women, hair loss is more diffuse (13). The development of such types of alopecia is widespread in the human population. The follicular automaton model can be applied readily to the study of various patterns of alopecia.

For simplicity, we represent human scalp by a square grid of 100×100 points (similar results would be obtained by simulating any larger grid—e.g., 300×300—with a number of nodes approaching the actual number of hair follicles, which is about 10^5 in nonalopecic subjects). It is known that male pattern baldness differentially affects frontal-vertex area and occipital area (10) and that hair variables in the occipital area of alopecic subjects are not significantly different compared with those of controls (14). Moreover, a shortening in the duration of A phase was noted when comparing alopecic with nonalopecic volunteers (5). Heterogeneity in the mean duration of the A phase might thus be suspected when comparing frontal-vertex area and occipital area.

To illustrate the effect of heterogeneity in mean duration of the A phase, μ_A, we consider in Fig. 5*A* a linear gradient such that μ_A varies from 7 months at the center of the grid up to 12 months at the extremity of its periphery. The circular contour lines showing the loci of similar mean duration of A phase are indicated in the (x,y) plane. These curves can be referred to as isomelics (from the Greek term $\mu\varepsilon\lambda\lambda o\nu$, for "future"), because follicles along them share the same duration in their (here, A) state, i.e., the same immediate future. A stronger gradient ranging from 3 to 20 months is considered in Fig. 5*F*. Finally, the effect of the latter gradient superimposed with two smaller gradients at the front ranging from 3 to 8 months is considered. Whereas the gradients in A phase are set from the beginning and do not change with time in Fig. 5 *A–C*, they could also appear and evolve over the course of time, as considered in Fig. 4*F*.

The results of the simulation by the follicular automaton model in the conditions specified in Fig. 5 *A–C* are represented for each gradient situation as a sequence of panels giving the number of cycles (n) performed in each node of the spatial grid, successively 10, 15, 20, and 25 years after initial time in which $n = 0$. Initial time typically corresponds to the situation at an age close to 20–25 years; in this initial, spatially homogeneous state, all follicles are considered as starting in A phase. The color code in Fig. 5 indicates that the follicles that have gone through 20 cycles or more are represented by an orange to red dot. If we assume that follicles die after performing 20 to 25 cycles, the orange-red areas in the figure correspond to zones of irreversible hair loss characterizing alopecia. In the conditions corresponding to Fig. 5*B*, the simulation indicates that the follicles near the center reach 20 cycles more rapidly because of shorter mean duration of A phase, because this duration progressively decreases from the periphery toward the center (the mean duration of T and L phases is supposed to be the same for all follicles, regardless of their location). In the conditions of Fig. 5*C*, the same effect is observed, additionally, in the two frontal triangular regions. For Fig. 5*A*, because the gradient in mean duration of A phase is more shallow and goes down to a value of only 8 (instead of 3) months near the center, we do not observe the formation of a central zone of follicles that have gone through 25 successive cycles after 25 years.

The final patterns represented in Fig. 5 are reminiscent of well known types of alopecia. Thus, the gradient situation in Fig. 5*A* gives rise to the appearance of diffuse (Ludwig-type) alopecia often encountered in women (13). The gradients considered in Fig. 5 *B* and *D* are associated with the onset of male pattern baldness [Hamilton type (ref. 10) of androgenetic alopecia]. Our results thus show that various patterns of alopecia can originate readily from the distribution of isomelic lines, which correspond here to a linear gradient in mean duration of A phase increasing

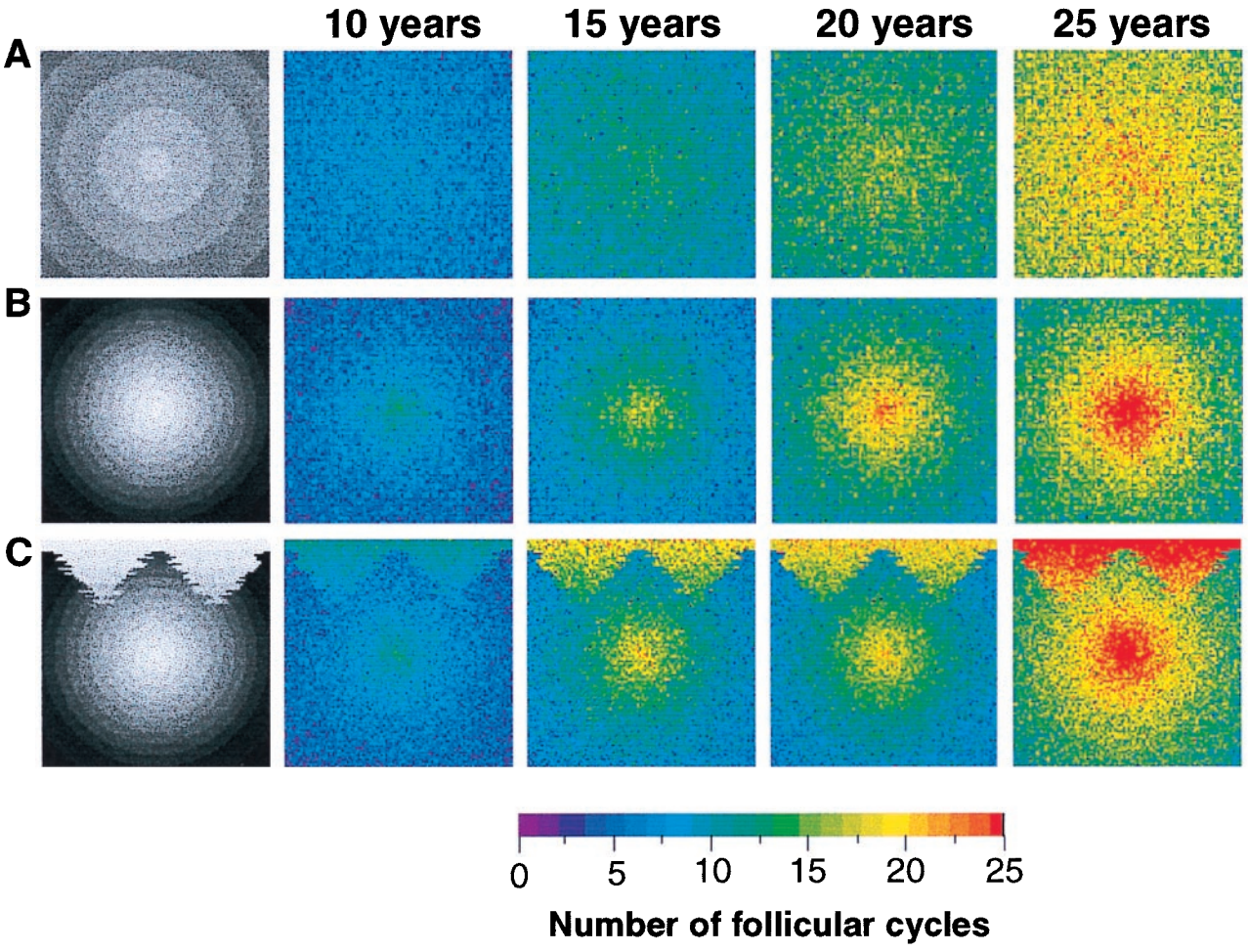

Fig. 5. Spatiotemporal evolution of a field of cycling hair follicles and patterns of alopecia. Each row shows a sequence of four spatial patterns of follicular growth (in colors) generated by the follicular automaton model at 5-year intervals, as a result of a particular spatial distribution (black and white panel) of mean durations of A phase (μ_A), in a field of 100 × 100 nodes representing a given scalp area (see text). The gray scale for the mean duration of A phase goes from white (μ_A = 3 months) to dark gray (μ_A = 20 months). In *A*, lines of same durations (*isomelic* lines) show that μ_A increases from 7 to 12 months from center to periphery. In *B*, the sharper gradient extends from 3 to 20 months. In *C*, the same gradient shown in *B* is superimposed with two small, triangular gradients extending symmetrically at the front, from 3 months at the top to 7 months toward the center. As indicated by the scale at the bottom of the figure, the color panels give the number of cycles performed by hair follicles. The color changes successively from blue to green, yellow, and red as the follicles go through 10, 15, 20, and 25 cycles or more. If we assume that follicles die after going through about 25 cycles, the areas turned red correspond to areas affected by hair loss. The initial follicular pattern (not shown), similar in each of the three cases considered, is homogeneously violet (0 cycle in each node of the grid). This initial condition corresponds, for example, to the situation seen in 20- to 30-year-old subjects. The final hair patterns shown 25 years after corresponds to a diffuse alopecia of the type commonly seen in woman (top row) or to well known types of androgenetic alopecia, reminiscent of male pattern baldness (median and bottom rows). Parameter values are (in months) μ_T = 3.0, σ_T = 1.0, μ_L = 4.0, σ_L = 3.0, with $\sigma_A = \mu_A$.

from the center (vertex) to the periphery, possibly superimposed with smaller gradients on the frontal area. More complicated scenarios involving a progressive decrease of μ_A with time, nonlinear gradients, or additional changes in the mean duration of T and L phases or in the critical number of cycles as a function of spatial location have also been considered and lead to the other graded patterns of androgenetic alopecia (10).

Discussion

Hair follicles are characterized by the cyclic nature of their development (1- 5). Growth occurs during the A phase and stops before entering T phase; the decayed follicle is replaced after an L phase. The goal of the present study was to propose a theoretical model simulating the dynamics of human hair cycles, based on the large amount of data collected over a period of 14 years on the characteristics of scalp hair cycles in a group of 10 human male volunteers. It is the collective spatiotemporal behavior of some 10^5 cycling follicles that governs the global evolution of human hair, including the commonly observed transition to various types of alopecia.

The model proposed herein, referred to as follicular automaton, is based on the assumption that each follicle, independently of its neighbors, undergoes cyclical transitions through A, T, and L phases, successively, before entering a new A phase or dying. The transitions possess a stochastic nature and occur according to a distribution of durations characteristic of each phase (Fig. 2). These distributions were determined from experimental observations, each of the three distributions for a given subject being associated with a mean and a variance. The time evolution of the follicular automaton is governed by a set of algorithmic rules. Application of these rules by successive iterations generates the time evolution of any number of hair follicles on a specified area of the scalp.

After showing that the automaton reproduces the typical dynamics of a single hair follicle (Fig. 3), we have considered the evolution of a field of independently cycling follicles. The model

reproduces faithfully the evolution toward a regime in which the fractions of follicles in A, T, or L phases fluctuate around steady-state or slowly drifting values (Fig. 4). The steady-state values depend on the mean duration of each of the three follicular phases. The model succeeds in reproducing the fluctuations seen in experimental observations that were carried out on a limited number of about 100 follicles, both in the case where the duration of the A phase remains constant (Fig. 4 *D* and *E*) or varies (Fig. 4*F*) over the course of time.

We have also applied the follicular automaton model to the study of spatial patterns that can arise over the course of time as a result of the heterogeneous distribution of follicular parameters and of the possible death of follicles after a critical number of cycles. The results shown in Fig. 5 indicate that structures reminiscent of well known patterns of androgenetic (10) or diffuse alopecia (13) readily arise from gradients in the mean duration of A phase (Fig. 5) that increase from the center to the periphery of a model scalp. Such gradients could be associated with spatial variations in molecular processes governing, for example, the synthesis of—or sensitivity to—the growth factors and other molecules active in the control of hair follicle cycling (15–18).

Based on a set of simple rules, the follicular automaton model therefore accounts qualitatively and quantitatively for a number of characteristics of human hair cycles. Moreover, the model can be used to determine the types of changes in biochemical parameters that underlie the transition to various patterns of androgenetic alopecia. This study further suggests that the independence of each follicle within a field of growing follicles and the variability in the duration of the A phase represent major determinants of the collective dynamics of human hair cycles.

We thank Dr. G. Lang for his continuous interest in this work, Dr. D. Saint-Léger for discussions, Dr. C. Bouillon for comments on the manuscript, and L'Oréal for financial support.

1. Kligman, A. M. (1959) *J. Invest. Dermatol.* **33,** 307–316.
2. Hardy, M. F. (1992) *Trends Genet.* **8,** 55–61.
3. Abell, E. (1994) in *Disorders of Hair Growth*, ed. Olsen, E. A. (McGraw–Hill, New York), pp. 1–19.
4. Stenn, K., Parimoo, S. & Prouty, S. M. (1998) in *Molecular Basis of Epithelial Appendage Morphogenesis*, ed. Chuong, C. M. (Landes, Austin, TX), pp. 111–130.
5. Courtois, M., Loussouarn, G., Hourseau, C. & Grollier, J. F. (1994) *Skin Pharmacol.* **7,** 84–89.
6. Courtois, M., Loussouarn, G., Hourseau, C. & Grollier, J. F. (1995) *Br. J. Dermatol.* **132,** 86–93.
7. Whiting, D. A. (1998) *Int. J. Dermatol.* **37,** 561–566.
8. Ishino, A., Uzuka, M., Tsuji, Y., Nakanishi, J., Hanzana, N. & Imamura, S. (1997) *J. Dermatol.* **24,** 758–764.
9. Headington, J. T. (1984) *Arch. Dermatol.* **120,** 449–456.
10. Hamilton, J. B. (1951) *Ann. N.Y. Acad. Sci.* **53,** 708–728.
11. Courtois, M., Loussouarn, G., Hourseau, C. & Grollier, J. F. (1996) *Br. J. Dermatol.* **134,** 47–54.
12. Ermentrout, G. B. & Edelstein-Keshet, L. (1993) *J. Theor. Biol.* **160,** 97–133.
13. Ludwig, E. (1977) *Br. J. Dermatol.* **97,** 247–254.
14. Rushton, D. H., Ransay, I. D., Norris, M. J. & Gilkes, J. J. H. (1991) *Clin. Exp. Dermatol.* **16,** 188–192.
15. Stenn, K. S., Prouty, S. M. & Seiberg, M. (1994) *J. Dermatol. Sci.* **7,** S109–S124.
16. Philpott, M. & Paus, R. (1998) in *Molecular Basis of Epithelial Appendage Morphogenesis*, ed. Chuong, C. M. (Landes, Austin, TX), pp. 75–110.
17. Sato, N., Leopold, P. L. & Crystal, R. G. (1999) *J. Clin. Invest.* **104,** 855–864.
18. Millar, S. E., Willert, K., Salinas, P. C., Roelink, H., Nusse, R., Sussman, D. J. & Barsh, G. S. (1999) *Dev. Biol.* **207,** 133–149.